

Transition of a Deep Eutectic Solution to Aqueous Solution: A Dynamical Perspective of the Dissolved Solute

Sushil S. Sakpal,[#] Samadhan H. Deshmukh,[#] Srijan Chatterjee, Deborin Ghosh, and Sayan Bagchi*



Cite This: *J. Phys. Chem. Lett.* 2021, 12, 8784–8789



Read Online

ACCESS |



Metrics & More

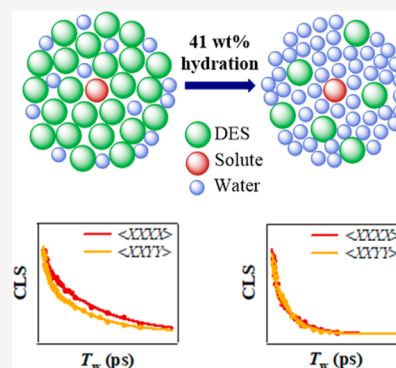


Article Recommendations



Supporting Information

ABSTRACT: Disruption of the deep eutectic solvent (DES) nanostructure around the dissolved solute upon addition of water is investigated by polarization-selective two-dimensional infrared spectroscopy and molecular dynamics simulations. The heterogeneous DES nanostructure around the solute is partially retained up to 41 wt % of added water, although water molecules are gradually incorporated in the solute's solvation shell even at lower hydration levels. Beyond 41 wt %, the solute is observed to be preferentially solvated by water. This composition denotes the upper hydration limit of the deep eutectic solvent above which the solute senses an aqueous solvation environment. Interestingly, our results indicate that the transition from a deep eutectic solvation environment to an aqueous one around the dissolved solute can happen at a hydration level lower than that reported for the “water in DES” to “DES in water” transition.



Fuelled by searching for environmentally friendly solvents for sustainable chemical processes, deep eutectic solvents (DESs) have emerged as green designer solvents with a wide range of applications.^{1–5} A typical DES consists of an HB acceptor (HBA) and an HB donor (HBD), mixed in the eutectic molar ratio.^{3,6–8} DES nanostructures, stabilized by intercomponent HB interactions, can be further tuned by the addition of cosolvents capable of disrupting the native HB networks.^{6–10} As water can act as both HBA and HBD, these neoteric solvents are highly water-miscible and hygroscopic.^{11,12} Recent reports demonstrate that water addition in the eutectic mixtures influences the DES nanostructures and consequently impacts their physicochemical properties.⁶ Trends in these properties suggest an upper limit of DES hydration, above which DES behaves like an aqueous solution.^{13–15}

Reline, composed of urea (HBD) and choline chloride (ChCl, HBA) in a 2:1 molar ratio, is one of the most widely studied DESs. This solvent has extensive use in biodiesel synthesis, surface coating, and enzymatic reactions.^{16–18} Owing to the hygroscopic nature of both urea and ChCl, the presence of water changes the macroscopic properties of reline and perturbs the DES nanostructure.¹⁹ Experimental and theoretical studies have reported water's effect on the physicochemical properties and molecular arrangement of reline.^{6,15,20–22} Notably, an unusual transition from an ionic mixture (“water in reline”) to an aqueous solution (“reline in water”) at 51 wt % water was recently reported by Hammond et al. using neutron diffraction experiments and empirical potential surface refinement (EPSR).⁸

Although various reports studied the disruption of reline nanostructure at certain hydration levels,^{6,7,9,15} all the studies focused on understanding the phenomenon from the solvent's perspective in the absence of any dissolved solute. The effect of increasing water content in reline from the solute's perspective has yet to be explored. A favorable arrangement of the DES components around the solute provides an ideal environment for applications like selective catalysis and efficient synthesis.² The disruption of the preferred molecular organization in the presence of water might perturb the favorable solute–reline interactions, limiting the use of reline in such applications. Furthermore, water is often intentionally added to improve the DES properties, for example, to lower viscosity.^{6,15} Does the solute sense the transition from a heterogeneous ionic mixture to an aqueous solution at the same water content reported by Hammond et al.? In other words, what is the hydration limit above which the interactions between the solute molecule and the DES components cease to exist?

Herein, we report the polarization-selective evolution of the solute's vibrational frequencies, which provides the answers to the questions mentioned above. We also perform molecular dynamics (MD) simulations on different reline–water systems in the solute's presence to obtain a molecular understanding of the solute–solvent interactions at different hydration levels.

Received: June 30, 2021

Published: September 7, 2021



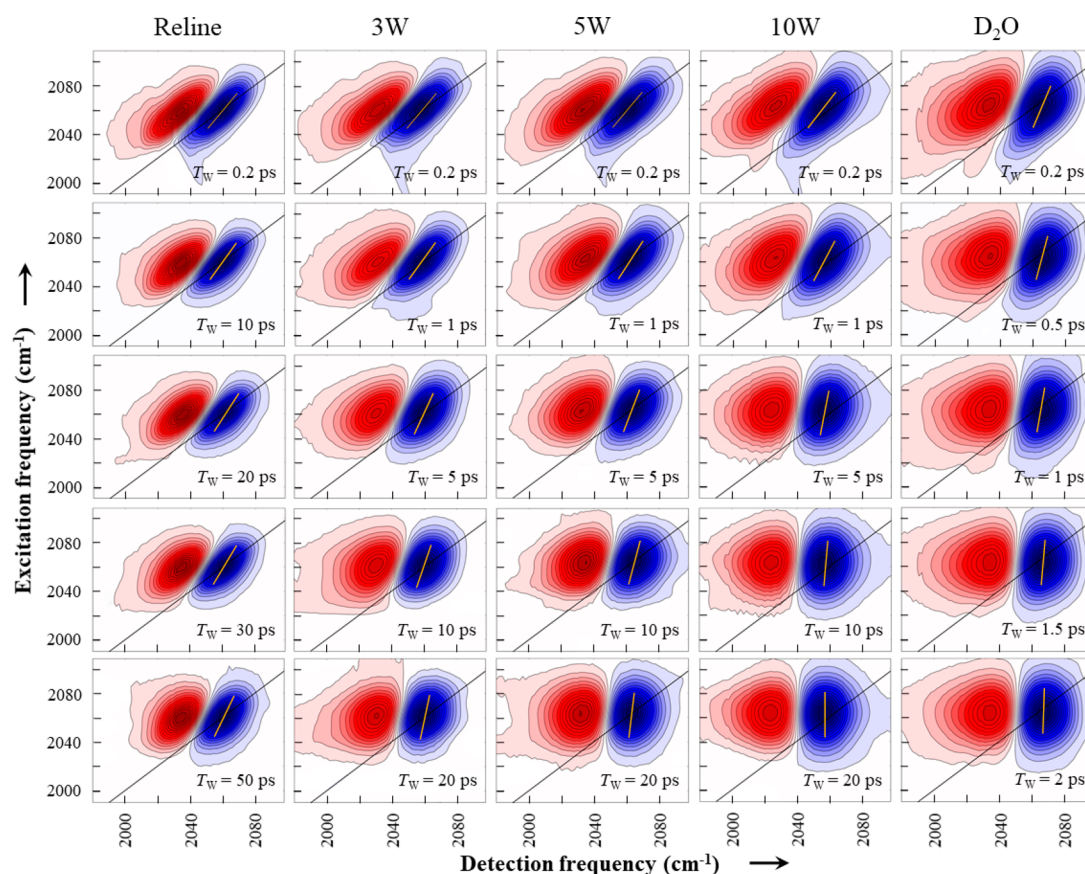


Figure 1. 2D IR spectra of SCN^- in reline, in reline–water (D_2O) mixtures, and in water (D_2O) at $\langle\text{XXXX}\rangle$ polarization condition. The peak pairs correspond to $\bar{\nu}_{\text{CN}}$. The water content increases from left to right. For a certain hydration level, T_w increases from top to bottom. The CLS is shown in each 2D IR spectrum with a yellow line.

The structural dynamics of the solvent produce frequency evolution within its inhomogeneously broadened vibrational bands. These dynamics are quantified by the frequency–frequency correlation function (FFCF) through time-dependent line shape analysis of two-dimensional infrared (2D IR) spectra.^{23,24} When dissolved in a relatively slow-moving solvent, the solute can reorient on a much faster timescale than the solvent’s complete structural evolution. The rapid reorientation of the solute contributes to a polarization selectivity of the frequency evolution over time, known as reorientation-induced spectral diffusion (RISD).²⁵ A recent report on room-temperature ionic liquids (RTILs) shows that polarization dependence of the solute’s FFCF can distinguish a slowly evolving environment from an aqueous solution.²³ Considering the gradual lowering of viscosity upon increasing water content in the DESs, polarization-selective 2D IR spectroscopy is suitable to identify the transition from a eutectic to an aqueous environment from the solute’s perspective. As thiocyanate is one of the common vibrational probes,^{26–29} we have performed polarization-selective 2D IR experiments on ammonium thiocyanate dissolved in reline and reline–water mixtures (Figures 1 and S1). We prepared a series of aqueous reline mixtures ($x\text{W}$) by mixing x (ranging from 0 to 15) moles of water (D_2O) with one mole of reline. Water–reline molar ratios ($x\text{W}$) of 3W, 5W, 10W, and 15W were used (the detailed weight % and mol % are given in Table S1 of the Supporting Information) as solvents along with neat reline and water.

In the 2D IR experiments, three ultrashort femtosecond pulses are focused on the sample at different time delays. The time delay between pulses 1 and 2 is τ , and that between 2 and 3 is T_w . Owing to the structural dynamics of the solvent molecules and the reorientation of the solute, the initial CN stretching frequencies of the solute change as a function of T_w . For a particular T_w , the 2D IR spectrum (Figures 1 and S1) correlates the initial solute frequencies after first pulse interaction (ω_τ , excitation frequencies) with the final solute frequencies after third pulse interaction (ω_t , detection frequencies). The blue peaks ($\omega_\tau \approx 2060 \text{ cm}^{-1}$, $\omega_t \approx 2060 \text{ cm}^{-1}$) correspond to $\nu = 0 \rightarrow 1$ transition and the red peaks ($\omega_\tau \approx 2060 \text{ cm}^{-1}$, $\omega_t \approx 2030 \text{ cm}^{-1}$) correspond to $\nu = 1 \rightarrow 2$ transitions, shifted by the vibrational anharmonicity along ω_t . The 2D IR peaks are diagonally elongated at a shorter T_w because of a greater correlation between the initial and the final CN frequencies. However, the correlation decreases with the evolution of frequencies over time, and the peaks gradually become upright with an increase in T_w . Figure 1 indicates that the peaks become upright at a shorter T_w as reline’s water content increases. As the faster structural dynamics of the solvent leads to a faster correlation decay, the T_w -dependent 2D IR spectra in different solvation environment are consistent with the decrease in the DES viscosity upon water addition (Table S2).

We have extracted the FFCF encoded in the T_w -dependent 2D IR spectra for two different polarization conditions, $\langle\text{XXXX}\rangle$ and $\langle\text{XXYY}\rangle$, in terms of the center line slope (CLS) decay²³ (Figure 2a–d and Tables S3 and S4). For

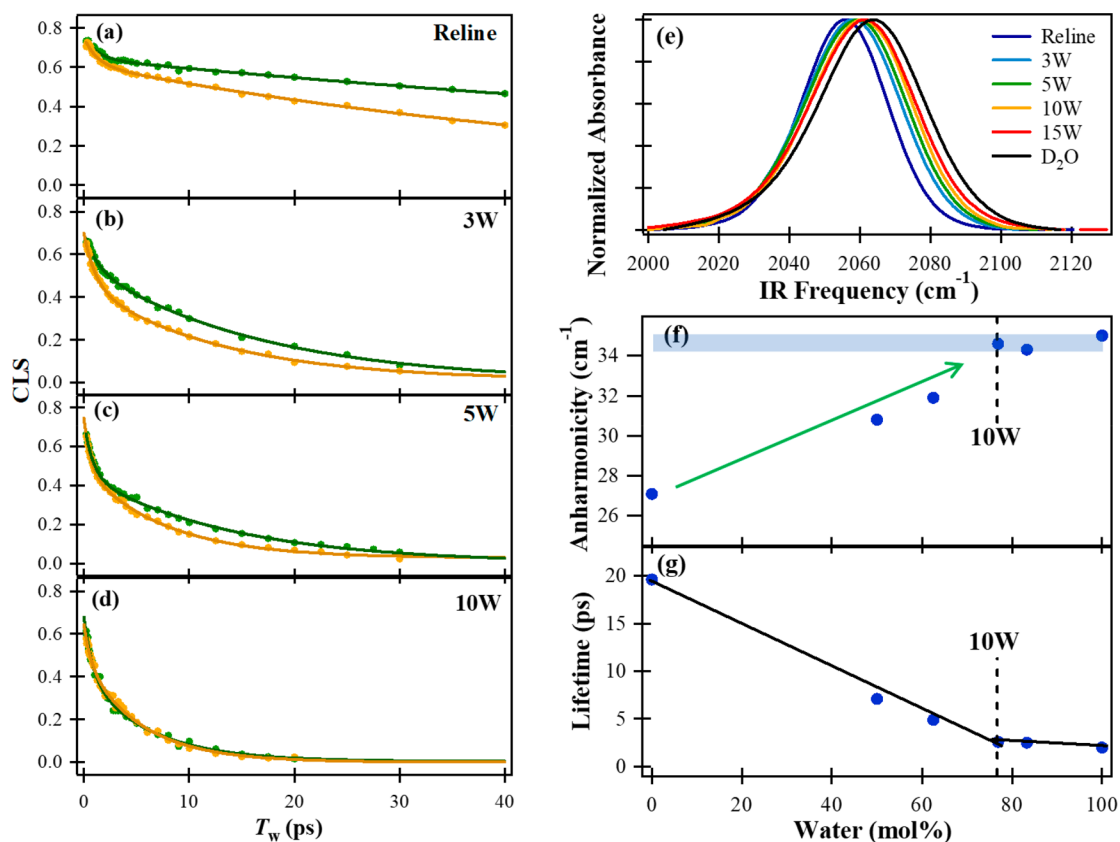


Figure 2. (a–d) CLS decay curves of SCN^- in reline and in reline–water mixtures for $\langle\text{XXXX}\rangle$ (green) and $\langle\text{XXYY}\rangle$ (yellow) polarization conditions. Polarization selectivity is observed for reline, 3W, and 5W. The CLS decays become identical at 10W within experimental error. (e) FTIR spectrum of ammonium thiocyanate in reline, in various reline– D_2O mixtures, and in neat D_2O . The peak maximum shows a gradual blue-shift with increasing hydration level of the solvent. (f) SCN^- anharmonicity in reline and reline– D_2O mixtures shows a gradual increase up to 10W (green arrow), beyond which the anharmonicity remains constant (shaded region) within experimental error bar. (g) SCN^- vibrational lifetime in reline and reline– H_2O mixtures suggests a nonmonotonic change in the solvation environment at 10W.

reline, the CLS for the $\langle\text{XXXX}\rangle$ polarization (green) shows a slower decay than that for the $\langle\text{XXYY}\rangle$ polarization (yellow). The polarization-selective CLS decays are also observed for 3W and 5W, although the difference in the decays becomes smaller with the increase in the water content. Interestingly, the CLS decays become identical for both $\langle\text{XXXX}\rangle$ and $\langle\text{XXYY}\rangle$ polarization conditions at 10W within experimental error. Further addition of water shows no polarization-dependence of the CLS decays.

We have analyzed the anisotropy decay kinetics of the different reline–water systems (Figure S2 and Table S5) to understand the origin of the polarization dependence of the CLS decays. The CLS decay timescales in both $\langle\text{XXXX}\rangle$ and $\langle\text{XXYY}\rangle$ polarization conditions are slower than that of the corresponding anisotropy decay timescales (~ 6 ps) for reline, 3W, and 5W. The CLS decays for 10W and above are either comparable to or faster than the anisotropy decays. These results strongly support that the polarization-selective CLS decays in Figure 2a–c arise from RISD, where the solute reorientation occurs without complete randomization of the DES structure. In a viscous solvent like reline, a component of the solvent structure contributing to the overall CN vibrational band can be considered static on the solute reorientation timescale, giving rise to the polarization selectivity.²³

The blue-shift in the CN IR peak (Figure 2e and Table S6) with increasing water content indicates an increment in solute–water HB interaction.³⁰ The decrease in the difference

between the $\langle\text{XXXX}\rangle$ and $\langle\text{XXYY}\rangle$ decays from reline to 5W arises because of the increase in the rapidly fluctuating (~ 1.5 ps)^{24,31} water molecules around the solute with increasing hydration. However, the polarization-selective decays at 3W and 5W demonstrate that the solute is still interacting with the slowly fluctuating reline through the transition dipole’s angular motion. In other words, the huge difference between the fluctuation timescales between reline and water implies that the polarization dependence arises because of the presence of DES components around the solute at these hydration levels. A plausible explanation toward the identical CLS decays at 10W is that the solute is predominantly solvated by the water molecules that fluctuate at a timescale faster than or comparable to the solute’s reorientation. Any further increase in the hydration level (up to neat water) would not further perturb the solvation shell of the solute, and the CLS decays remain identical, independent of polarization conditions. From the solute’s perspective, the transition from a deep eutectic solution (solute–DES interaction) to an aqueous solution (only solute–water interaction) occurs at $\sim 10\text{W}$ (41 wt % water).

However, it is to be noted that the merging of the CLS decays alone cannot provide a molecular picture of the transition in the solvation environment. In fact, although the CLS decays become identical at 10W in both the polarization conditions, the CLS decay timescales continue to gradually accelerate beyond 10W (Tables S3 and S4) with further

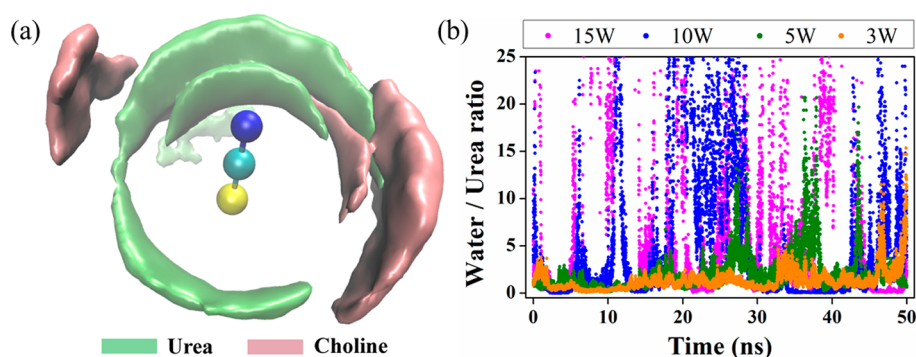


Figure 3. (a) Spatial distribution function (SDF) of urea and choline around SCN^- in neat reline. (b) Graph of water/urea ratio within 10 Å of the SCN^- vs time in different reline–water mixtures.

increase in the water content. This gradual acceleration might imply that the local solvation continues to evolve beyond 10W and thereby contradicts our hypothesis that an aqueous environment around the solute is formed at 41 wt % water. To verify the transition from a deep eutectic solution to an aqueous solution, we have further looked into complementary experimental observables and MD simulations.

To obtain better insights about the local solvation, we have looked into the vibrational anharmonicity. Previous studies of thiocyanate reported that proximity to the cations usually results in the lowering of the vibrational anharmonicity.^{32–35} We have estimated the anharmonicity to gradually increase from $\sim 27 \text{ cm}^{-1}$ in reline to $\sim 35 \text{ cm}^{-1}$ at 10W (Table S7 and Figure 2f). However, the anharmonicity does not change for 15W and neat water within the experimental error limit. This trend in the anharmonicity is in agreement with the gradual replacement of the ionic DES components around the solute by water molecules up to 10W.

We have also performed MD simulations to further probe the local solvation around the solute. Although earlier simulation reports investigated the bulk nature of the reline–water interaction at different hydration levels,^{7,9,15} the local solvation around a solute was not explored. We have calculated the spatial distribution function (SDF) which provides the three-dimensional density distribution of urea and choline around the solute in neat reline. Figure 3a indicates that, although choline contains a hydroxyl group which can directly interact with the CN, solute–urea interaction is preferred over solute–choline interaction in neat reline. Previous studies of thiocyanate in aqueous solutions reported viscosity-dependent slowdown of the solute rotational dynamics due to interactions with small cations with high charge density.³³ The preferential interaction of the solute with urea over choline (albeit a much larger cation) shows that local environment of the solute plays a larger role in DES than the macroscopic viscosity. We have also computed the water/urea and water/choline ratios within 5 and 10 Å of the solute in different reline–water mixtures. The ratios, averaged along the trajectories, show an increase with increasing water content of reline (Table S8). However, a very interesting phenomenon is observed when the ratios are plotted as a function of time. Figure 3b indicates that the water/urea ratio gradually increases from 3W and reaches the maximum value at 10W. Beyond 10W, this ratio remains constant. However, the ratios keep switching between high and low values, thereby indicating a solvent exchange process where the water molecules around the solute are replaced by the reline components from time to time. The frequency of the

solvent exchange increases with increasing water content. It has previously been reported that molecular exchange between solvent components slow down the solvation dynamics and results in a slower spectral diffusion in an aqueous mixture than in water.^{36–38} Thus, the simulation results show that the experimental CLS decay timescales can be interpreted on the basis of solvent exchange. Even though the solute senses an overall aqueous environment at 10W, the decrease in the mole fraction of the reline components in the outer solvation shell with increase in water content plausibly leads to a faster solvent exchange and thereby an acceleration of the CLS decay timescales.

Overall, our computational results indicate that although water interacts with the solute at 5W, a considerable number of heterogeneous reline constituents persist in the thiocyanate solvation shell. At 10W and above, solute–solvent interactions predominantly arise from thiocyanate–water interactions, subsequently decreasing the heterogeneity around the solute. This molecular picture was further validated from experiments using the vibrational lifetimes (T_1) and the CLS values at a short T_w ($\sim 200 \text{ fs}$) (Table S9 and Tables S3 and S4, respectively).

We have measured T_1 for different reline– D_2O mixtures using pump–probe spectroscopy (Figure S3 and Table S9). In pure reline, T_1 of the CN vibrational mode is $\sim 20 \text{ ps}$. The T_1 values in all other mixtures are constant ($\sim 11 \text{ ps}$) within experimental error. The CN vibration's coupling with the resonant water mode (bending + libration) through HB interaction can explain the invariability of vibrational relaxation timescales at all hydration levels.³⁹ The constant T_1 indicates the presence of water in the solute solvation shell, even at 3W. As the thiocyanate vibrational lifetime in H_2O is much shorter than that in D_2O ,⁴⁰ T_1 in reline– H_2O might be a more sensitive probe of solute hydration. We have additionally measured T_1 for different reline– H_2O mixtures (Table S10). Our results show that T_1 of the CN vibrational mode in H_2O gradually decreases with increase in water content up to 10W. Beyond 10W, T_1 is almost constant within the experimental error. This trend in the lifetime indicates that the solute is predominantly solvated by water molecules at 10W. The initial amplitude of the CLS at a very short T_w is a measure of the dynamical heterogeneity around the solute. The decrease in the initial CLS amplitude (Figure 2a–d and Tables S3 and S4) from reline to 10W implies a gradual replacement of slowly moving DES components by fast fluctuating water molecules in the thiocyanate solvation shell (Figure 4).

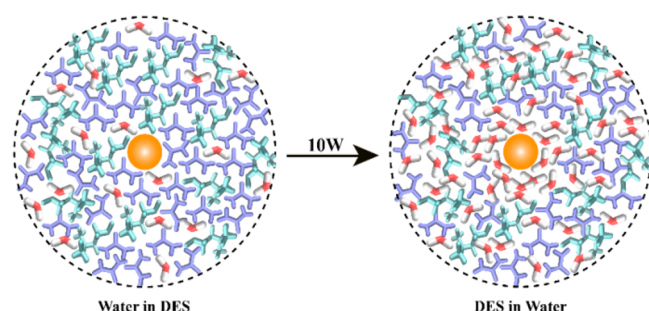


Figure 4. Schematic diagram for “Water in DES” and “DES in Water” transition. The solute molecule is represented by an orange sphere. The solute–water interactions replace all the solute–DES interactions at 10W, thereby creating a neat water-like environment around the solute.

In summary, we provide an upper hydration limit of reline beyond which the solute experiences a water-like environment. Interestingly, our results demonstrate that this upper hydration limit (41 wt % water or 10W) is considerably lower than the limit proposed by Hammond et al. (51 wt % water or 15W) from the neutron diffraction study.⁸ However, the diffraction results provided us an upper hydration limit from the solvent’s perspective, i.e., when each reline constituent (choline cation, chloride anion, and urea) is solvated by water. The polarization-selective 2D IR results demonstrate that the solute may experience an aqueous environment much before water solvates all the reline constituents. Further, this report illustrates that polarization dependence of the structural dynamics could identify when the solute experiences a transition from the heterogeneous DES environment to an aqueous solution. For a wide range of applications, researchers are presently exploiting hydration as a tool to overcome the limitations of green solvents like DESs and RTILs.^{4,7,15,41} This study opens up an avenue to investigate similar transitions from the solute’s perspective for viscous green solvents with varying constituents.

■ ASSOCIATED CONTENT

SI Supporting Information

The Supporting Information is available free of charge at <https://pubs.acs.org/doi/10.1021/acs.jpcllett.1c02118>.

Synthesis of DES and preparation of DES–water mixtures, IR and 2D IR spectroscopy, molecular dynamics simulations, additional figures and tables (PDF)

■ AUTHOR INFORMATION

Corresponding Author

Sayan Bagchi – Physical and Materials Chemistry Division, National Chemical Laboratory (CSIR-NCL), Pune 411008, India; Academy of Scientific and Innovative Research (AcSIR), Ghaziabad 201002, India; orcid.org/0000-0001-6932-3113; Email: s.bagchi@ncl.res.in

Authors

Sushil S. Sakpal – Physical and Materials Chemistry Division, National Chemical Laboratory (CSIR-NCL), Pune 411008, India; Academy of Scientific and Innovative Research (AcSIR), Ghaziabad 201002, India

Samadhan H. Deshmukh – Physical and Materials Chemistry Division, National Chemical Laboratory (CSIR-NCL), Pune

411008, India; Academy of Scientific and Innovative Research (AcSIR), Ghaziabad 201002, India

Srijan Chatterjee – Physical and Materials Chemistry Division, National Chemical Laboratory (CSIR-NCL), Pune 411008, India; Academy of Scientific and Innovative Research (AcSIR), Ghaziabad 201002, India; orcid.org/0000-0001-9701-4158

Deborin Ghosh – Physical and Materials Chemistry Division, National Chemical Laboratory (CSIR-NCL), Pune 411008, India

Complete contact information is available at:

<https://pubs.acs.org/10.1021/acs.jpcllett.1c02118>

Author Contributions

*S.S.S. and S.H.D. contributed equally to this work.

Notes

The authors declare no competing financial interest.

■ ACKNOWLEDGMENTS

S.B. thanks CSIR-NCL and SERB, India (SR/S2/RJN-142/2012 and EMR/2016/000576) for financial support. D.G. acknowledges SERB India (PDF/2018/000046) for financial support. The support and the resources provided by “PARAM Brahma Facility” under the National Supercomputing Mission, Government of India at the Indian Institute of Science Education and Research (IISER) Pune are gratefully acknowledged. S.S.S. acknowledges UGC and S.H.D acknowledges CSIR for research fellowships.

■ REFERENCES

- (1) Smith, E. L.; Abbott, A. P.; Ryder, K. S. Deep Eutectic Solvents (DESs) and Their Applications. *Chem. Rev.* **2014**, *114*, 11060–11082.
- (2) Wagle, D. V.; Zhao, H.; Baker, G. A. Deep eutectic solvents: sustainable media for nanoscale and functional materials. *Acc. Chem. Res.* **2014**, *47*, 2299–2308.
- (3) Hammond, O. S.; Li, H.; Westermann, C.; Al-Murshedi, A. Y. M.; Endres, F.; Abbott, A. P.; Warr, G. G.; Edler, K. J.; Atkin, R. Nanostructure of the deep eutectic solvent/platinum electrode interface as a function of potential and water content. *Nanoscale Horiz.* **2019**, *4*, 158–168.
- (4) Liao, H.-G.; Jiang, Y.-X.; Zhou, Z.-Y.; Chen, S.-P.; Sun, S.-G. Shape-Controlled Synthesis of Gold Nanoparticles in Deep Eutectic Solvents for Studies of Structure–Functionality Relationships in Electrocatalysis. *Angew. Chem., Int. Ed.* **2008**, *47*, 9100–9103.
- (5) Hammond, O. S.; Edler, K. J.; Bowron, D. T.; Torrente-Murciano, L. Deep eutectic-solvothermal synthesis of nanostructured ceria. *Nat. Commun.* **2017**, *8*, 14150.
- (6) Hammond, O. S.; Bowron, D. T.; Edler, K. J. The Effect of Water upon Deep Eutectic Solvent Nanostructure: An Unusual Transition from Ionic Mixture to Aqueous Solution. *Angew. Chem., Int. Ed.* **2017**, *56*, 9782–9785.
- (7) Kumari, P.; Shobhna; Kaur, S.; Kashyap, H. K. Influence of Hydration on the Structure of Reline Deep Eutectic Solvent: A Molecular Dynamics Study. *ACS Omega* **2018**, *3*, 15246–15255.
- (8) Ma, C.; Laaksonen, A.; Liu, C.; Lu, X.; Ji, X. The peculiar effect of water on ionic liquids and deep eutectic solvents. *Chem. Soc. Rev.* **2018**, *47*, 8685–8720.
- (9) Sarkar, S.; Maity, A.; Chakrabarti, R. Microscopic structural features of water in aqueous–reline mixtures of varying compositions. *Phys. Chem. Chem. Phys.* **2021**, *23*, 3779–3793.
- (10) Shah, D.; Mansurov, U.; Mjalli, F. S. Intermolecular interactions and solvation effects of dimethylsulfoxide on type III deep eutectic solvents. *Phys. Chem. Chem. Phys.* **2019**, *21*, 17200–17208.

- (11) Dugoni, G. C.; Di Pietro, M. E.; Ferro, M.; Castiglione, F.; Ruellan, S.; Moufawad, T.; Moura, L.; Costa Gomes, M. F.; Fourmentin, S.; Mele, A. Effect of Water on Deep Eutectic Solvent/ β -Cyclodextrin Systems. *ACS Sustainable Chem. Eng.* **2019**, *7*, 7277–7285.
- (12) Durand, E.; Lecomte, J.; Barea, B.; Dubreucq, E.; Lortie, R.; Villeneuve, P. Evaluation of deep eutectic solvent–water binary mixtures for lipase-catalyzed lipophilization of phenolic acids. *Green Chem.* **2013**, *15*, 2275–2282.
- (13) Gutierrez, M. a. C.; Ferrer, M. a. L.; Mateo, C. R.; del Monte, F. Freeze-Drying of Aqueous Solutions of Deep Eutectic Solvents: A Suitable Approach to Deep Eutectic Suspensions of Self-Assembled Structures. *Langmuir* **2009**, *25*, 5509–5515.
- (14) Passos, H.; Tavares, D. J. P.; Ferreira, A. M.; Freire, M. G.; Coutinho, J. A. P. Are Aqueous Biphasic Systems Composed of Deep Eutectic Solvents Ternary or Quaternary Systems. *ACS Sustainable Chem. Eng.* **2016**, *4*, 2881–2886.
- (15) Shah, D.; Mjalli, F. S. Effect of water on the thermo-physical properties of Reline: An experimental and molecular simulation based approach. *Phys. Chem. Chem. Phys.* **2014**, *16*, 23900–23907.
- (16) Zhang, Q.; De Oliveira Vigier, K.; Royer, S.; Jerome, F. Deep eutectic solvents: syntheses, properties and applications. *Chem. Soc. Rev.* **2012**, *41*, 7108–7146.
- (17) Bucko, M.; Culliton, D.; Betts, A. J.; Bajat, J. B. The electrochemical deposition of Zn–Mn coating from choline chloride–urea deep eutectic solvent. *Trans. Inst. Met. Finish.* **2017**, *95*, 60–64.
- (18) Liao, Y. S.; Chen, P. Y.; Sun, I. W. Electrochemical study and recovery of Pb using 1:2 choline chloride/urea deep eutectic solvent: A variety of Pb species PbSO_4 , PbO_2 , and PbO exhibits the analogous thermodynamic behavior. *Electrochim. Acta* **2016**, *214*, 265–275.
- (19) Agieienko, V.; Buchner, R. Densities, Viscosities, and Electrical Conductivities of Pure Anhydrous Reline and Its Mixtures with Water in the Temperature Range (293.15 to 338.15) K. *J. Chem. Eng. Data* **2019**, *64*, 4763–4774.
- (20) D'Agostino, C.; Gladden, L. F.; Mantle, M. D.; Abbott, A. P.; Ahmed, E. I.; Al-Murshedi, A. Y. M.; Harris, R. C. Molecular and ionic diffusion in aqueous – deep eutectic solvent mixtures: probing intermolecular interactions using PFG NMR. *Phys. Chem. Chem. Phys.* **2015**, *17*, 15297–15304.
- (21) Fetisov, E. O.; Harwood, D. B.; Kuo, I. F. W.; Warrag, S. E. E.; Kroon, M. C.; Peters, C. J.; Siepmann, J. I. First-Principles Molecular Dynamics Study of a Deep Eutectic Solvent: Choline Chloride/Urea and Its Mixture with Water. *J. Phys. Chem. B* **2018**, *122*, 1245–1254.
- (22) Posada, E.; Lopez-Salas, N.; Jimenez Rioboo, R. J.; Ferrer, M. L.; Gutierrez, M. C.; del Monte, F. Reline aqueous solutions behaving as liquid mixtures of H-bonded co-solvents: microphase segregation and formation of co-continuous structures as indicated by Brillouin and ^1H NMR spectroscopies. *Phys. Chem. Chem. Phys.* **2017**, *19*, 17103–17110.
- (23) Tamimi, A.; Bailey, H. E.; Fayer, M. D. Alkyl Chain Length Dependence of the Dynamics and Structure in the Ionic Regions of Room-Temperature Ionic Liquids. *J. Phys. Chem. B* **2016**, *120*, 7488–7501.
- (24) Kwak, K.; Park, S.; Finkelstein, I. J.; Fayer, M. D. Frequency-frequency correlation functions and apodization in two-dimensional infrared vibrational echo spectroscopy: a new approach. *J. Chem. Phys.* **2007**, *127*, 124503–124517.
- (25) Kramer, P. L.; Nishida, J.; Fayer, M. D. Separation of experimental 2D IR frequency-frequency correlation functions into structural and reorientation-induced contributions. *J. Chem. Phys.* **2015**, *143*, 124505–124516.
- (26) Bian, H.; Wen, X.; Li, J.; Chen, H.; Han, S.; Sun, X.; Song, J.; Zhuang, W.; Zheng, J. Ion clustering in aqueous solutions probed with vibrational energy transfer. *Proc. Natl. Acad. Sci. U. S. A.* **2011**, *108*, 4737–4742.
- (27) Li, J.; Bian, H.; Chen, H.; Wen, X.; Hoang, B. T.; Zheng, J. Ion Association in Aqueous Solutions Probed through Vibrational Energy Transfers among Cation, Anion, and Water Molecules. *J. Phys. Chem. B* **2013**, *117*, 4274–4283.
- (28) Chen, H.; Wen, X.; Guo, X.; Zheng, J. Intermolecular vibrational energy transfers in liquids and solids. *Phys. Chem. Chem. Phys.* **2014**, *16*, 13995–14014.
- (29) Cui, Y.; Fulfer, K. D.; Ma, J.; Weldeghiorghis, T. K.; Kuroda, D. G. Solvation dynamics of an ionic probe in choline chloride-based deep eutectic solvents. *Phys. Chem. Chem. Phys.* **2016**, *18*, 31471–31479.
- (30) Deb, P.; Haldar, T.; Kashid, S. M.; Banerjee, S.; Chakrabarty, S.; Bagchi, S. Correlating Nitrile IR Frequencies to Local Electrostatics Quantifies Noncovalent Interactions of Peptides and Proteins. *J. Phys. Chem. B* **2016**, *120*, 4034–4046.
- (31) Kramer, P. L.; Nishida, J.; Giammanco, C. H.; Tamimi, A.; Fayer, M. D. Observation and theory of reorientation-induced spectral diffusion in polarization-selective 2D IR spectroscopy. *J. Chem. Phys.* **2015**, *142*, 184505–184508.
- (32) Roy, V. P.; Kubarych, K. J. Interfacial Hydration Dynamics in Cationic Micelles Using 2D-IR and NMR. *J. Phys. Chem. B* **2017**, *121*, 9621–9630.
- (33) Bian, H.; Chen, H.; Zhang, Q.; Li, J.; Wen, X.; Zhuang, W.; Zheng, J. Cation Effects on Rotational Dynamics of Anions and Water Molecules in Alkali (Li^+ , Na^+ , K^+ , Cs^+) Thiocyanate (SCN^-) Aqueous Solutions. *J. Phys. Chem. B* **2013**, *117*, 7972–7984.
- (34) Park, S.; Ji, M.; Gaffney, K. J. Ligand Exchange Dynamics in Aqueous Solution Studied with 2DIR Spectroscopy. *J. Phys. Chem. B* **2010**, *114*, 6693–6702.
- (35) Kiefer, L. M.; Kubarych, K. J. NOESY-Like 2D-IR Spectroscopy Reveals Non-Gaussian Dynamics. *J. Phys. Chem. Lett.* **2016**, *7*, 3819–3824.
- (36) Dunbar, J. A.; Arthur, E. J.; White, A. M.; Kubarych, K. J. Ultrafast 2D-IR and Simulation Investigations of Preferential Solvation and Cosolvent Exchange Dynamics. *J. Phys. Chem. B* **2015**, *119*, 6271–6279.
- (37) Kiefer, L. M.; Kubarych, K. J. Solvent exchange in preformed photocatalyst-donor precursor complexes determines efficiency. *Chem. Sci.* **2018**, *9*, 1527–1533.
- (38) Kashid, S. M.; Jin, G. Y.; Chakrabarty, S.; Kim, Y. S.; Bagchi, S. Two-Dimensional Infrared Spectroscopy Reveals Cosolvent-Composition-Dependent Crossover in Intermolecular Hydrogen-Bond Dynamics. *J. Phys. Chem. Lett.* **2017**, *8*, 1604–1609.
- (39) Hamm, P.; Lim, M.; Hochstrasser, R. M. Vibrational energy relaxation of the cyanide ion in water. *J. Chem. Phys.* **1997**, *107*, 10523–10531.
- (40) Czurlok, D.; Gleim, J.; Lindner, J.; Vöhringer, P. Vibrational Energy Relaxation of Thiocyanate Ions in Liquid-to-Supercritical Light and Heavy Water. A Fermi's Golden Rule Analysis. *J. Phys. Chem. Lett.* **2014**, *5*, 3373–3379.
- (41) Dong, J. Y.; Hsu, Y. J.; Wong, D. S. H.; Lu, S. Y. J. Growth of ZnO Nanostructures with Controllable Morphology Using a Facile Green Antisolvent Method. *J. Phys. Chem. C* **2010**, *114*, 8867–8872.